

## Nanostructured ZnO: Building Blocks for Nanoscale Devices

Z. FAN AND J. G. LU

*Department of Chemical Engineering and Materials Science &  
Department of Electrical Engineering and Computer Science  
University of California, Irvine, CA 92697, USA*

ZnO is attracting intensive attention for its versatile applications in transparent electronics, UV emitter, piezoelectric devices, chemical sensor and spin electronics. As one of the direct wide band gap semiconductors, it has advantages over GaN due to its larger exciton binding energy, better lattice match on heteroepitaxial growth and availability of single crystal substrate. Large effort has been invested in the growth of nanostructured ZnO to explore its potentials for nanoscale device applications. ZnO nanobelts, nanowires, nanorings, and nanohelices demonstrate the diversity of ZnO nanostructures family. This review presents recent research on ZnO nanostructures. Issues of synthesis methods, optical, electrical, gas sensing and magnetic properties are summarized. These progresses constitute the basis for developing future applications in nanoscale electronics, optoelectronics, chemical sensor and spintronics.

*Keywords:* wide band gap semiconductor; nanostructures; transparent electronics; UV emission; chemical sensor; spintronics

### 1. Introduction

Zinc oxide (ZnO) is one of the most important functional oxide semiconductors because of its unique properties and potential applications in manifold fields, such as transparent electronics, ultraviolet (UV) light emitter, surface acoustic wave (SAW) devices and spin electronics. Invisible thin film transistors (TFTs) using ZnO as an active channel achieve much higher field effect mobility ( $7 \text{ cm}^2/\text{V}\cdot\text{s}$ ) than amorphous silicon TFTs ( $0.5 \text{ cm}^2/\text{V}\cdot\text{s}$ ) [1-3]. ZnO has been proposed to be a more promising UV emitting phosphor than GaN because of its large exciton binding energy (60 meV), larger than the thermal energy at room temperature. This lowers the UV lasing threshold and yields higher UV emitting efficiency at room temperature [4]. Excitonic emissions have been observed from the photoluminescence spectra of ZnO nanorods [5]. Large scale vertically aligned ZnO nanorods have been synthesized, demonstrating the potential of fabricating nano-optoelectronics arrays [6]. SAW filters using ZnO films have already been used for video and radio frequency circuits. Piezoelectric ZnO thin film has been fabricated into ultrasonic transducer arrays operating at 100 MHz [7]. Holes mediated ferromagnetic ordering in bulk ZnO by introducing manganese (Mn) as dopant has been predicted theoretically [8] and reported recently [9]. Vanadium doped *n*-type ZnO films also demonstrate a Currie temperature above room temperature [10]. Due to these remarkable

physical properties and the motivation of the device miniaturization trend, large efforts have been focused on nanoscale ZnO materials to fabricate high density, high speed, low power devices. An assortment of ZnO nanostructures, such as nanorods, nanowires, and nanorings, have been successfully grown via a variety of methods including chemical vapor deposition, thermal evaporation, and electrodeposition [11-14]. These nanostructures have been subjected to electrical transport [15,16], UV emission [4,17], gas sensing [18], and ferromagnetic doping [9,19,20] studies, and considerable progresses have been achieved. In this paper, recent research achievements on ZnO nanostructures are reviewed, summarizing studies on their synthesis methods, structural, mechanical, electrical, sensing, optical, and magnetic properties.

## 2. Synthesis and characterization of ZnO nanostructures

ZnO nanostructures are usually obtained via a vapor transport process. Depending on the synthesis condition variations in temperature, catalyst, and composition of source materials, a wide range of nanostructures has been obtained. Using a vapor-solid process, complex ZnO nanostructures such as nanohelices, nanorings and nanobelts were synthesized by Kong *et al.* [21] (Fig. 1a). In this process, ZnO powder was decomposed into  $Zn^{2+}$  and  $O^{2-}$  at  $\sim 1400$  °C then transported by Ar carrier gas to a low temperature zone ( $\sim 400$  °C), and nanostructures were formed on a collecting chip. In a similar vapor transport and condensation process reported by Ren *et al.* [22, 23], hierarchical ZnO nanostructures were grown by mixing ZnO,  $In_2O_3$  and graphite powder and heated up to 820-870 °C. A simplified method to achieve nanowires, nanoribbons and nanorods was reported by Yao *et al.* [13]: ZnO powder was mixed with graphite and heated to 1100 °C then cooled down, nanostructures were found to form on the wall of the furnace. These synthesis methods utilize the vapor-solid (VS) mechanism, in which ZnO nanostructures are formed by condensing directly from vapor phase. Although diverse nanostructures can be obtained, this method provides less control on the geometry of ZnO nanostructures. Controlled growth of ZnO nanowires has been achieved by using various nanoparticles or nanoclusters as catalysts, such as Au [24, 25], Cu [26], and Co [27]. In these cases, ZnO and carbon powder are usually used as source material and a vapor-liquid-solid (VLS) growth mechanism governs the synthesis. In the VLS mechanism, the catalyst nanoparticles become liquid droplet under reaction temperature. The reactant Zn vapor generated by carbon thermal reduction of ZnO powder is transported to the catalyst nano-droplets and form Zn-catalyst alloy. In the meantime, ZnO forms as a result of the reaction between Zn and CO/CO<sub>2</sub>. Upon supersaturation, ZnO nanowires grow from the droplets. Recently we have found that this synthesis process can be further simplified by directly heating pure Zn powder in low concentration oxygen environment (2%) using Au nanoparticles as catalysts [28]. The as-synthesized nanowires show high quality and they grow along (0001) direction, as indicated in Figs. 1b & 1c. The advantage of using nanoparticles as catalysts lies in the better control of the nanostructure growth. Based on the VLS mechanism, the diameter of nanowire can be tuned by using different size nanoparticle catalysts. Yang *et al.* reported achievements of ZnO nanowires growth in controlling the position, orientation, diameter and density [4]. In their method, (110) plane sapphire was used as an epitaxial substrate to obtain vertically grown ZnO nanowires along the (001) direction (Fig. 1d). Besides using sapphire as epitaxy substrate, anodic alumina membranes (AAM) was utilized

as templates to obtain highly ordered ZnO nanowire arrays [14,15]. These well-controlled synthesis methods pave the way to the integration of ZnO nanostructures for future large scale device applications.

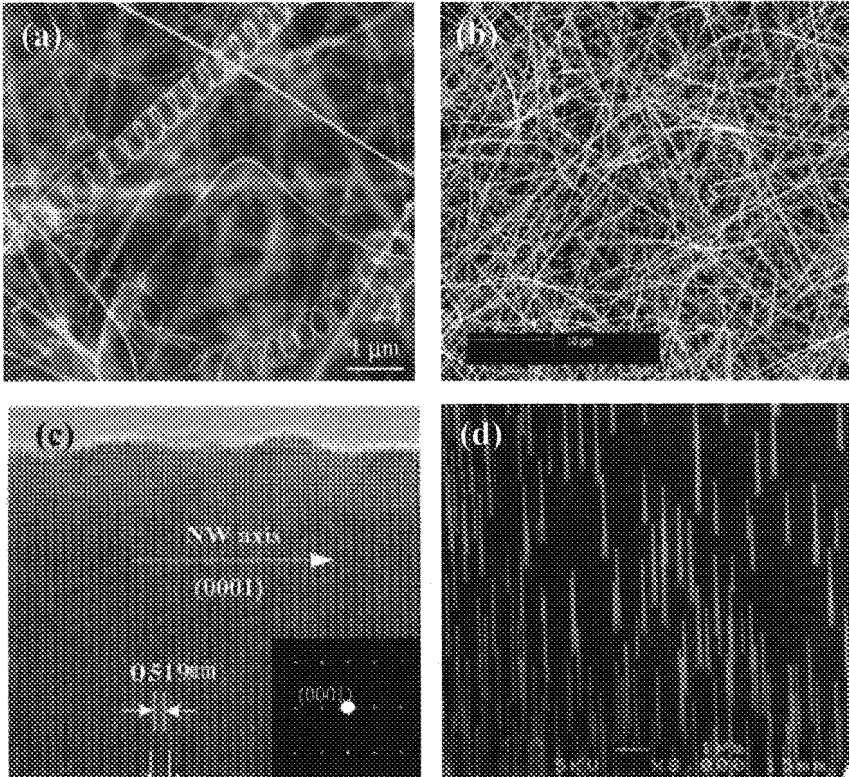


Fig. 1. (a) ZnO nanohelix structures grown via Vapor-Solid process. (reprint permission from ref. [21]) (b) ZnO nanowires grown via VLS process. (c) High resolution TEM image of a ZnO nanowire shows growth direction along (0001). (d) Vertical aligned ZnO nanowires array on sapphire substrate. (reprint permission from ref. [4])

### 3. Mechanical properties of ZnO nanostructures

Understanding the fundamental physical properties is central to the rational design of functional devices. Investigation on individual ZnO nanostructures is critical to their applications in nanoelectronic devices and systems. Direct measurement of mechanical behavior of individual nanostructures is rather challenging since the traditional measurement method for bulk material does not apply. Based on an electric-field-induced resonant excitation, Bai [29] *et al.* characterized the bending modulus of ZnO nanobelts using transmission electron microscopy (TEM). In this method, a special TEM sample holder was

made to apply an oscillating electric field between a ZnO nanobelt and a fixed electrode. This electric field drove the vibration of the nanobelt, and resonant oscillation was achieved by tuning the driving frequency, as depicted in Fig. 2. Following the classical elasticity theory, bending modulus was calculated and shown in Table 1. ZnO nanobelt demonstrates to be a promising material for nanoresonator and nanocantilever. Its small size renders improved sensitivity compared with conventional cantilever fabricated by microtechnology. Hughes [30] *et al.* reported manipulation of ZnO nanobelt to the desired length and position. This could lead to the usage of nanobelt as highly sensitive atomic force microscopy probe.

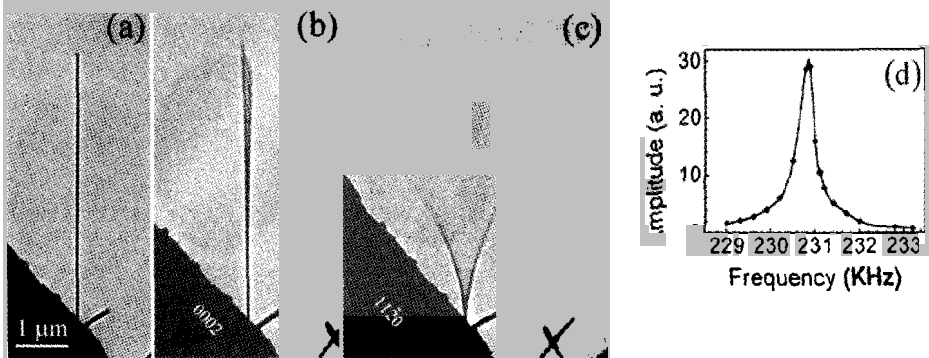


Fig. 2 TEM images of a ZnO nanobelt at (a) stationary (b) the first harmonic resonance in x (thickness) direction,  $\nu_x = 622$  KHz, (c) the first harmonic resonance in y (width) direction,  $\nu_y = 691$  KHz. (d) Resonance peak of a ZnO nanobelt. (reprint permission from ref. [29])

Table 1. Bending modulus of ZnO nanobelts.  $E_x$  and  $E_y$  represents for the modulus along thickness and width direction. (reprint permission from ref. [29])

Nanobelt	Length $L$ ( $\mu\text{m}$ ) ( $\pm 0.05$ )	Width $W$ ( $\mu\text{m}$ ) ( $\pm 1$ )	Thickness $T$ ( $\text{nm}$ ) ( $\pm 1$ )	Fundamental frequency (kHz)			Bending modulus (GPa)		
				$W/T$	$\nu_{x1}$	$\nu_{y1}$	$\nu_{y1}/\nu_{x1}$	$E_x$	$E_y$
1	8.25	55	33	1.7	232	373	1.6	$46.6 \pm 0.6$	$50.1 \pm 0.6$
2	4.73	28	19	1.5	396	576	1.4	$44.3 \pm 1.3$	$45.5 \pm 2.9$
3	4.07	31	20	1.6	662	958	1.4	$56.3 \pm 0.9$	$64.6 \pm 2.3$
4	8.90	44	39	1.1	210	231	1.1	$37.9 \pm 0.6$	$39.9 \pm 1.2$

#### 4. Electrical properties

Electrical transport measurements have been performed on individual ZnO nanowires and nanorods [16, 31-33]. Fan [31] *et al.* configured single ZnO nanowires as field effect transistors using photolithography. Nanowires synthesized by CVD method were dispersed first in isopropanol alcohol to form nanowires suspension, then deposited onto  $\text{SiO}_2/\text{Si}$  substrate. Photolithography was used to define contact electrodes array. Degenerately doped Si substrate was used to serve as a back gate, and the neighboring electrodes contacting a nanowire function as source and drain. Due to native defects such as oxygen vacancies and

zinc interstitials, ZnO nanowires are reported to be *n*-type semiconductor. Figure 3a shows *I-V* characteristics under different back gate voltages. Well defined transfer characteristic is shown in Fig. 3b. Carrier concentration and mobility are derived from the transfer characteristic of the nanowire transistor to be  $\sim 10^7 \text{ cm}^{-1}$  and  $\sim 17 \text{ cm}^2/\text{V}\cdot\text{s}$ , respectively. It is worth noting that the CVD grown ZnO nanostructures are usually single crystalline, rendering them superior electrical property than polycrystalline thin film. For example, an electron field effect mobility of  $7 \text{ cm}^2/\text{V}\cdot\text{s}$  is regarded quite high for ZnO thin film transistors [2]. However, single crystalline ZnO nanowires showed much higher mobility, as Chang *et al.* had reported an electron mobility of  $80 \text{ cm}^2/\text{V}\cdot\text{s}$ . This indicates that the ZnO nanostructures based device can achieve a faster operation speed than their thin film counterpart. Furthermore, using a uniquely designed synthesis setup, one can modify the carrier concentration and mobility of the nanowires (Fig. 3c), providing a way to tune the electrical property of ZnO nanowires [28].

The major impediment of ZnO for broad electronics and photonics applications rests with the difficulty of *p*-type doping. Several *p*-type doping efforts have been reported, with a Ga and N codoping method, low resistivity ( $0.5 \Omega\text{cm}$ ) *p*-type ZnO thin film was obtained [34]. Look *et al.* reported nitrogen-doped *p*-type ZnO obtained by molecular beam epitaxy with a hole mobility of  $2 \text{ cm}^2/\text{V}\cdot\text{s}$  [35]. Kim *et al.* reported phosphorus-doped *p*-type ZnO with a thermal activation process [36]. Successful *p*-type doping for ZnO nanostructures will greatly enhance their potential applications for nanoscale electronics and optoelectronics. *P*-type and *n*-type ZnO nanowires can serve as *p-n* junction diodes and light emitting diodes (LED). And field effect transistors (FET) fabricated from them can constitute complementary logic circuits. Combined with their optical cavity effect, electrically driven nanowire laser can be potentially implemented. An attempt to make intramolecular *p-n* junction on ZnO nanowires was performed by Liu *et al* [15]. In this case, anodic aluminum membrane was used as a porous template with pore size around 40 nm. A two step vapor transport growth was applied and boron was introduced as the *p*-type dopant in the first step. Consequently, the *I-V* characteristics demonstrated rectifying behavior due to the intramolecular *p-n* junction in the nanowire.

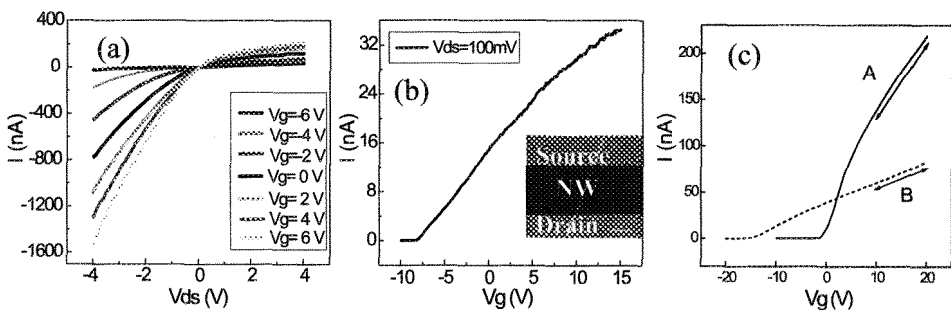


Fig. 3 (a) *I-V* curves of a ZnO nanowire FET from  $V_g = -6\text{V}$  to  $6\text{V}$ ; (b) Transfer characteristic of a ZnO nanowire FET (inset); (c) Transfer characteristics of two nanowires with different carrier concentration and carrier mobility. Nanowire A has a mobility of  $80 \text{ cm}^2/\text{V}\cdot\text{s}$  and carrier concentration  $\sim 10^6 \text{ cm}^{-1}$ ; and nanowire B has a mobility of  $22 \text{ cm}^2/\text{V}\cdot\text{s}$  and carrier concentration  $\sim 10^7 \text{ cm}^{-1}$ .

## 5. Electron field emission from vertical aligned ZnO nanostructures

Quasi-one-dimensional (Q1D) nanomaterial with sharp tip is a natural candidate for electron field emission. In fact, field emission from vertical aligned ZnO nanoneedles and nanowires have been investigated by many groups [27, 37-39]. Tseng [37] *et al.* grew needle-like ZnO nanowires on Ga-doped ZnO film at 550°C, the as-grown nanowires showed well-aligned vertical structure as shown in Fig. 4a. These nanowires were subject to field emission measurement, the turn-on field was found to be  $\sim 18$  V/ $\mu\text{m}$  at a current density of  $0.01 \mu\text{A}/\text{cm}^2$ , and the emission current could reach  $0.1 \text{ mA}/\text{cm}^2$  at  $24$  V/ $\mu\text{m}$ , as shown in Fig. 4b. Lee [27] *et al.* reported better results for ZnO nanowires synthesized at low temperature. They obtained a turn-on field of  $6$  V/ $\mu\text{m}$  at a current density of  $0.1 \mu\text{A}/\text{cm}^2$ , and the emission current reached  $1 \text{ mA}/\text{cm}^2$  at  $11$  V/ $\mu\text{m}$ , which could provide sufficient brightness to flat panel display.

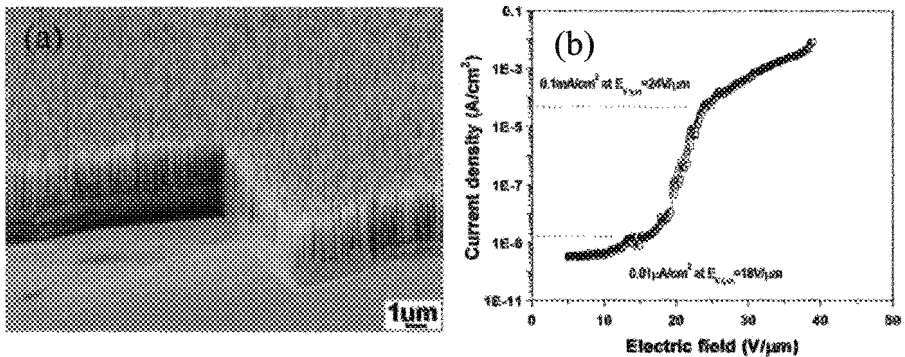


Fig. 4 (a) Vertically aligned ZnO nanowires on Ga-doped ZnO film; (b) Emission current-voltage characteristics of ZnO nanowires. (reprint permission from ref. [37])

## 6. Chemical sensing and hydrogen storage with ZnO Nanostructures

Oxygen vacancies on metal-oxide surfaces are electrically and chemically active. These vacancies function as *n*-type donors, often significantly increase the conductivity of oxide. Upon adsorption of charge accepting analytes at the vacancy sites, such as  $\text{NO}_2$  and  $\text{O}_2$ , electrons will be depleted from the conduction band, leading to a reduced conductivity of the *n*-type oxide. On the other hand, molecules that react with surface oxygen, such as  $\text{CO}$  and  $\text{H}_2$ , would react with surface adsorbed oxygen and remove it, leading to an increase in conductivity. Most metal-oxide gas sensors operate based on this principle. As one of the major materials for solid state gas sensor, bulk and thin films of ZnO have been proposed for  $\text{CO}$  [40],  $\text{NH}_3$  [41], alcohol [42] and  $\text{H}_2$  [43] sensing under elevated temperature ( $\sim 400$  °C). From the aspect of sensing performance, quasi-one-dimensional (Q1D) ZnO, such as nanowires and nanorods, is expected to be superior than its thin film counterpart. When their diameter is small and comparable to the Debye length, chemisorption induced surface states virtually affect the electronic structure of the entire channel, thus render Q1D ZnO higher sensitivity than thin film. In addition, ZnO nanowires and nanorods can be configured as

either two terminal sensing devices or as FETs in which an external electric field can be utilized to tune the sensing property. Recently, Wan [18] *et al.* fabricated ZnO nanowires gas sensor using microelectromechanical system technology. Massive nanowires were placed between Pt interdigitating electrodes. Under an operation temperature of 300 °C, the resistance of nanowires significantly decreases upon exposure to ethanol (Fig. 5a). Electrical transport studies show that O<sub>2</sub> ambient has considerable effect on the ZnO nanowires [16, 31]. Fan *et al.* discussed the relationship between oxygen pressure and ZnO nanowire FET performance [31]. It is shown that ZnO nanowires have fairly good sensitivity to O<sub>2</sub> (Fig. 5b). In addition, it is observed that the sensitivity is a function of back gate potential, *i.e.*, above gate threshold voltage of FET, sensitivity increases with decreasing gate voltage (Fig. 5b inset). This implies that the gate voltage can be used to adjust the sensitivity range. In addition, the large surface-to-volume ratio of nanowires not only results in their enhanced gas sensing performance, but also facilitates potential hydrogen storage property. Wan [44] *et al.* investigated hydrogen storage characteristics under room temperature. The highest storage of 0.83 wt% was achieved at a pressure of 3.03 MPa. In this work, it was suggested that hydrogen storage was due to not only surface adsorption but also the incorporation of H<sub>2</sub> into the crystal interstitial sites.

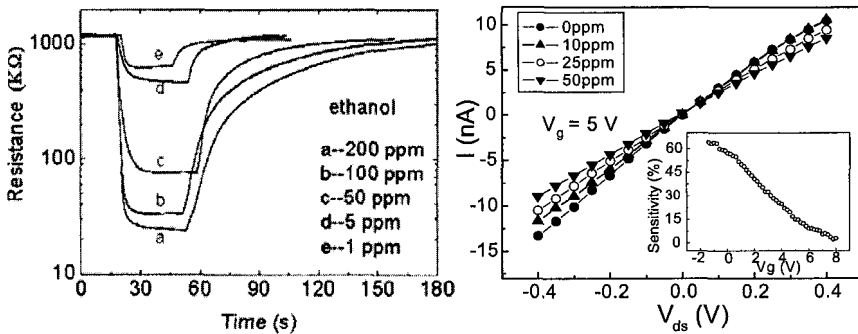


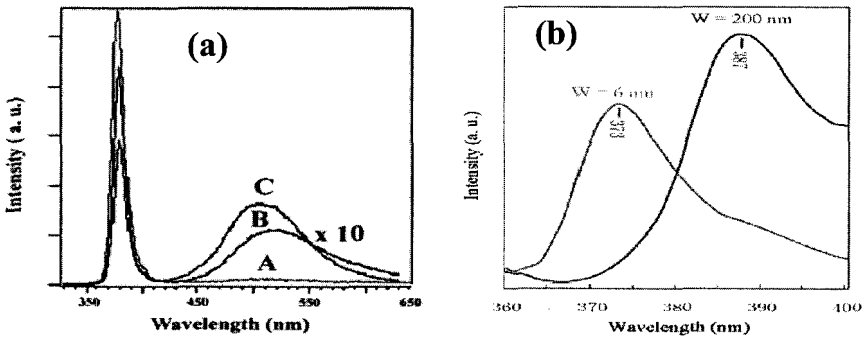
Fig. 5 (a) Response of ZnO nanowires upon exposure to ethanol with concentration of 1-200 ppm at 300 °C (reprint permission from ref. [16]); (b) I-V curves of a ZnO nanowire under 0-50 ppm O<sub>2</sub>. Inset: gate potential dependence of sensitivity under 10 ppm O<sub>2</sub>.

## 7. Optical properties

Intrinsic optical properties of ZnO nanostructures are being intensively studied for implementing photonic devices. Photoluminescence (PL) spectra of ZnO nanostructures have been extensively reported [4, 45-48]. Strong emission peak at 380 nm due to band to band transition and green-yellow emission band related to oxygen vacancy are observed, as shown in Fig. 6a. These results are consistent with those of bulk ZnO. Interestingly, the green emission intensity increases with decreasing nanowires diameter. This observation is attributed to the larger surface-to-volume ratio of thinner nanowires favoring a higher level of surface oxygen vacancy [4]. Recently, Fan *et al.* observed red luminescence attributed to

doubly ionized oxygen vacancies [49]. In addition, as one of the characteristics of nanoscale systems, quantum confinement was observed to cause a blue shift in the near UV emission peak [45] in ZnO nanobelts, as illustrated in Fig. 6b. PL spectra show that ZnO nanowire is a promising material for UV emitting, while its UV lasing property is of more significance and interest. Huang *et al.* [50] and Liu *et al.* [17] reported room temperature UV lasing from ordered ZnO nanowires array (Figs. 6c & 6d). 40 kW/cm<sup>2</sup> and 100 kW/cm<sup>2</sup> lasing power thresholds were reported and the higher threshold was attributed to larger defect concentration present in the wires. As pointed out in ref. 50, the advantages of ZnO nanowire lasers are that the excitonic recombination lowers the threshold of lasing, and in addition quantum confinement yields a substantial density of states at the band edges and enhances radiative recombination.

In addition, well-faceted nanowires form natural resonance cavities, as shown in Fig. 6b. Recently, Law *et al.* reported using ZnO nanowires as subwavelength optical waveguide [51]. Optically excited light emission was guided by ZnO nanowire into SnO<sub>2</sub> nanoribbon (Fig. 6e). These findings demonstrate that ZnO nanostructures can be the potential building blocks for integrated optoelectronic circuits. Besides UV emitting and lasing, effort on utilizing ZnO nanowires for UV photodetection and optical switching have been reported by Kind *et al.* [52]. Defect states related visible wavelength detection and polarized photodetection of ZnO nanowires were also observed [49] (Fig. 6f). Photocurrent is maximized when incident light is polarized parallel to nanowire long axis. This behavior is one of the characteristics of Q1D systems and makes them promising application in high contrast polarizer. From the photoconductivity measurements of ZnO nanowires, it is found that the presence of O<sub>2</sub> has crucial effect on the photoresponse [16, 49, 53], *i.e.* O<sub>2</sub> surface adsorption on the nanowires could greatly expedite the photocurrent relaxation rate. As shown in Fig. 6g, the photocurrent relaxation time is around 8 s in air but hours in vacuum. It was suggested that photoresponse of ZnO nanowire depends on the desorption-adsorption process of O<sub>2</sub>. Upon illumination, photo-generated holes discharge surface chemisorbed O<sub>2</sub> through surface electron-hole recombination, while the photo-generated electrons significantly increase the conductivity. When illumination is switched off, O<sub>2</sub> molecules re-adsorb onto nanowire surface and reduce electron concentration.



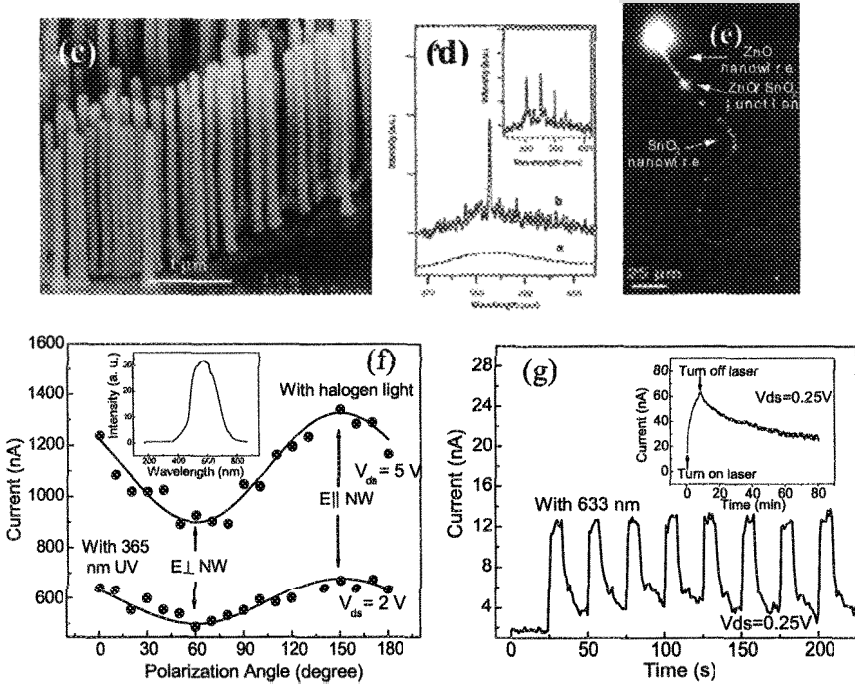


Fig. 6 (a) Photoluminescence spectrum of ZnO nanowires with diameter of 100 nm (A), 50 nm (B) and 25 nm (C) show near UV emission at 380 nm and green-yellow emission band. (reprint permission from ref. [4]) (b) PL spectra of 6 and 200 nm wide ZnO nanobelts show a blue shift of the emission peak. (reprint permission from ref. [45]) (c) Vertical aligned ZnO nanowires array on sapphire substrate used for light emission. (reprint permission from ref. [50]) (d) Emission spectra from nanowire array for optical pumping power below (line a) and above (line b, c) lasing threshold. The pumping power are 20, 100, 150 kW/cm<sup>2</sup>, respectively. (reprint permission from ref. [50]) (e) A PL image of a ZnO nanowire guiding light into a SnO<sub>2</sub> nanoribbon. (reprint permission from ref. [51]) (f) Polarized photodetection of both UV (365 nm) and visible light show that nanowire conductance is maximized when incident light is polarized parallel to the nanowire axis. (g) Nanowire photoresponse to 633 nm laser in air compared to that in vacuum (inset).

## 8. ZnO nanostructure for spintronics devices

Recently, diluted magnetic semiconductors (DMS) are attracting more and more research effort because spin-polarized DMS can accomplish efficient spin injection. It is found that ZnO is a promising host material for ferromagnetic doping. Room temperature holes mediated ferromagnetic ordering in bulk ZnO by introducing manganese (Mn) as dopant has been predicted theoretically [8] and observed by Sharma *et al.* in ZnO thin film [9]. Ferromagnetism was also observed when Co [54] and Fe [20, 55] were used as dopants. The

effort of growing ferromagnetic  $\text{Zn}_{1-x}\text{Mn}_x\text{O}$  ( $x=0.13$ ) nanowires with Currie temperature of 37 K was reported by Chang *et al.* [56] and shown in Fig. 7. The nanowires were synthesized via a vapor phase evaporation method. Because of its wide band gap, ferromagnetic ZnO is regarded as an excellent material for short wavelength magneto-optical devices [57]. These studies will pave the way for using magnetic ZnO nanowires as nanoscale spin-based devices, such as spin valves and spin FETs, with the ultimate goal of manipulating a single electron spin rather than the charge as in more conventional devices.

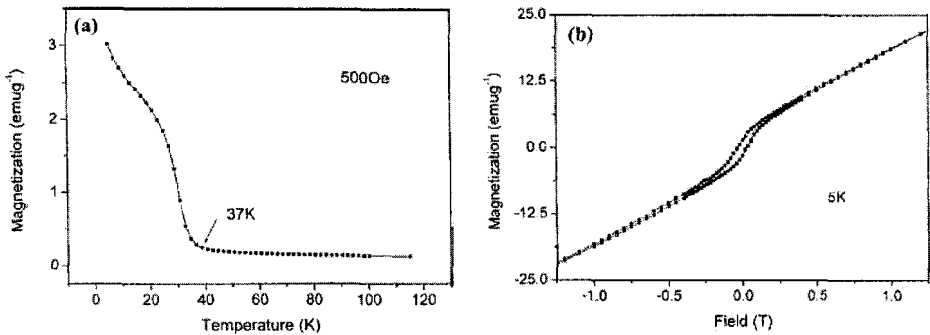


Fig. 7 (a) Temperature dependent magnetization curve of  $\text{Zn}_{1-x}\text{Mn}_x\text{O}$  ( $x=0.13$ ) nanowire at 500 Oe field shows Currie temperature of 37K. (b) Magnetization-Field hysteresis loop obtained at 5 K demonstrates ferromagnetism by Mn doping. (reprint permission from ref. [56])

## 9. Summary and future prospects

ZnO offers tremendous potential in providing electronic, photonic, and spin-based functionality. Encouraging progresses on the related research have been achieved as reviewed in this article. There are still important issues waiting to be further investigated, such as growing *p*-type ZnO nanowires and fabricating nanostructured *p-n* junction for electrically driven nano LED or laser. Integration of ZnO nanostructures for large scale device applications is another significant issue. Continuous effort will be dedicated to achieving high device density with accessibility to individual nanodevices. Obtaining room temperature ferromagnetism in ZnO nanostructures will greatly advance future research on ZnO based nanoscale spintronics devices.

## References

1. J. Nishii, F.M. Hossain, S. Takagi, T. Aita, K. Saikusa, Y. Ohmaki, I. Ohkubo, S. Kishimoto, A. Ohtomo, T. Fukumura, F. Matsukura, Y. Ohno, H. Koinuma, H. Ohno, and M. Kawasaki, "High Mobility Thin Film Transistors with Transparent ZnO Channels", *Jpn. J. Appl. Phys.* Vol. 42, pp.L347-L349, 2003.
2. F. M. Hossain, J. Nishii, S. Takagi, T. Sugihara, A. Ohtomo, T. Fukumura, H. Koinuma, H. Ohno, M. Kawasaki, "Modeling of grain boundary barrier modulation in ZnO invisible thin film transistors", *Physica E*, vol. 21, pp.911-915, 2004.
3. B.J. Norris, J. Anderson, J.F. Wager, D.A. Kszler, "Spin-coated zinc oxide transparent transistors", *J. Phys. D: Appl. Phys.* 36, pp.L105-107 (2003)
4. P. Yang, H. Yan, S. Mao, R. Russo, J. Johnson, R. Saykally, N. Morris, J. Pham, R. He, H.-J. Choi, "Controlled Growth of ZnO Nanowires and Their Optical Properties", *Adv. Mater.*, vol. 12, No. 5, pp.323-331, 2002.
5. W.I. Park, Y.H. Jun, S.W. Jung, and G. Yi, "Excitonic emissions observed in ZnO single crystal nanorods", *Appl. Phys. Lett.*, 82, pp.964-966, 2003.
6. X. Wang, C.J. Summers, and Z.L. Wang, "Large-scale hexagonal-patterned growth of aligned ZnO nanorods for nano-optoelectronics and Nanosensor Arrays", *Nano Lett.*, 4, pp.423-426, 2004.
7. Y. Ito, K. Kushida, K. Sugawara, and H. Takeuchi, "A 100-MHz ultrasonic transducer array using ZnO thin films", *IEEE Trans. Ultrasonics, Ferroelectrics, and Frequency Control*, Vol. 42, No. 2, pp.316-324, 1995.
8. T. Dietl, "Ferromagnetic semiconductors", *Semicond. Sci. Technol.*, vol. 17, pp.377-392, 2002.
9. P. Sharma, A. Gupta, K. V. Rao, F. J. Owens, R. Sharma, R. Ahuja, J. M. Osorio, B. Johansson, G. A. Gehring, "Ferromagnetism above room temperature in bulk and transparent thin films of Mn-doped ZnO", *Nature Mater.*, vol.2, pp.673-677, 2003.
10. H. Saeki, H. Tabata, T. Kawai, "Magnetic and electric properties of vanadium doped ZnO films", *Solid State Commun.*, vol. 120, pp. 439-443, 2001.
11. Z. L. Wang, "Nanostructures of Zinc Oxide", *Materialstoday*, pp. 26-33, June 2004.
12. P. X. Gao, Y. Ding, Z. L. Wang, "Crystallographic Orientation-Aligned ZnO Nanorods Grown by a Tin Catalyst", *Nano. Lett.*, vol. 3, No. 9, pp. 1315-1320, 2003.
13. B. D. Yao, Y. F. Chan, N. Wang, "Formation of ZnO nanostructures by a simple way of thermal evaporation", *Appl. Phys. Lett.*, vol. 81, No. 4, pp. 757-759, 2002.
14. Y. Li, G. S. Cheng, L. D. Zhang, "Fabrication of highly ordered ZnO nanowire arrays in anodic alumina membranes", *J. Mater. Res.*, vol. 15, No. 11, pp.2305-2308, 2000.
15. C. H. Liu, W. C. Yiu, F. C. K. Au, J. X. Ding, C. S. Lee, S. T. Lee, "Electrical properties of zinc oxide nanowires and intramolecular p-n junctions", *Appl. Phys. Lett.*, vol. 83 No. 15, pp. 3168-3170, 2003
16. Q. H. Li, Q. Wan, Y. X. Liang, T. H. Wang, "Electronic Transport through individual ZnO nanowires", *Appl. Phys. Lett.*, vol. 84, No. 22, pp. 4556-4558, 2004.
17. C. Liu, J. A. Zapien, Y. Yao, X. Meng, C. S. Lee, S. Fan, Y. Lifshitz, S. T. Lee, "High-Density, Ordered Ultraviolet Light-Emitting ZnO Nanowire Arrays", *Adv. Mater.*,

- vol. 15, No. 10, pp.838-841, 2003.
18. Q. Wan, Q. H. Li, Y. J. Chen, T. H. Wang, X. L. He, J. P. Li, C. L. Lin, "Fabrication and ethanol sensing characteristics of ZnO nanowire gas sensors", *Appl. Phys. Lett.*, vol. 84, No. 18, pp. 3654-3656, 2004.
  19. N. A. Theodoropoulou, A. F. Hebard, D. P. Norton, J. D. Budai, L. A. Boatner, J. S. Lee, Z. G. Khim, Y. D. Park, M. E. Overberg, S. J. Pearton, R. G. Wilson, "Ferromagnetism in Co- and Mn-doped ZnO", vol. 47, pp.2231-2235, 2003.
  20. S.-J. Han, J. W. Song, C.-H. Yang, S. H. Park, J.-H. Park, Y. H. Jeong, K. W. Rhie, "A key to room-temperature ferromagnetism in Fe-doped ZnO: Cu", *Appl. Phys. Lett.*, vol. 81, No. 22, pp. 4212-4214, 2002.
  21. X. Y. Kong, Z. L. Wang, "Spontaneous Polarization-Induced Nanohelices, Nanosprings, and Nanorings of Piezoelectric Nanobelts", *Nano. Lett.*, vol. 3, No. 12, pp.1625-1631, 2003.
  22. J. Y. Lao, J. G. Wen, Z. F. Ren, "Hierarchical ZnO Nanostructures", *Nano. Lett.*, vol. 2, No. 11, pp.1287-1291, 2002.
  23. J. G. Wen, J. Y. Lao, D. Z. Wang, T. M. Kyaw, Y. L. Foo, and Z. F. Ren, "Self-assembly of Semiconducting Oxide Nanowires, Nanorods, and Nanoribbons", *Chem. Phys. Lett.*, 372, pp. 717-722, 2003.
  24. M. H. Huang, Y. Wu, H. Feick, N. Tran, E. Weber, P. Yang, "Catalytic Growth of Zinc Oxide Nanowires by Vapor Transport", *Adv. Mater.*, vol. 13, pp. 113-116, 2001.
  25. Q. X. Zhao, M. Millander, R. E. Morjan, Q.-H. Hu, E. E. B. Campbell, "Optical recombination of ZnO nanowires grown on sapphire and Si substrate", *Appl. Phys. Lett.*, vol. 83, pp. 165-167, 2003.
  26. S. Y. Li, C. Y. Lee, T. Y. Tseng, "Copper-catalyzed ZnO nanowires on silicon (100) grown by vapor-liquid-solid process", *J. Cryst. Growth*, vol. 247, pp. 357-362, 2003.
  27. C. J. Lee, T. J. Lee, S. C. Lyu, Y. Zhang, H. Ruh, H. J. Lee, "Field emission from well-aligned zinc oxide nanowire grown at low temperature", *Appl. Phys. Lett.*, vol. 81, pp. 3648-3650, 2002.
  28. P. Chang, Z. Fan, W. Tseng, D. Wang, W. Chiou, J. Hong, J. G. Lu, "ZnO Nanowires Synthesized by Vapor Trapping CVD method", *Chem. Mater.*, to be published.
  29. X. D. Bai, P. X. Gao, Z. L. Wang, E. G. Wang, "Dual-mode mechanical resonance of individual ZnO nanobelts", *Appl. Phys. Lett.*, vol. 82, pp.4806-4808, 2003.
  30. W. L. Hughes, Z. L. Wang, "Nanobelts as nanocantilever", *Appl. Phys. Lett.*, vol. 82, pp.2886-2888, 2003.
  31. Z. Fan, D. Wang, P. Chang, W. Tseng, J. G. Lu, "ZnO Nanowire Field Effect Transistor and Oxygen Sensing Property", *Appl. Phys. Lett.*, to be published.
  32. Y. W. Heo, L. C. Tien, D. P. Norton, B. S. Kang, F. Ren, B. P. Gila, S. J. Pearton, "Electrical transport properties of single ZnO nanorods", *Appl. Phys. Lett.*, vol. 85, pp. 2002-2005, 2004.
  33. M. S. Arnold, P. Avouris, Z. W. Pan, Z. L. Wang, "Field-Effect Transistors Based on Single Semiconducting Oxide Nanobelts", *J. Phys. Chem. B*, vol. 107, pp. 659-663, 2003.
  34. M. Joseph, H. Tabata, H. Saeki, K. Ueda, T. Kawai, "Fabrication of the low-resistive p-type ZnO by codoping method", *Physica B*, vol. 302-303, pp. 140-148, 2001.
  35. D. C. Look, D. C. Reynolds, C. W. Litton, R. L. Jones, D. B. Eason, G. Cantwell,

- “Characterization of homoepitaxial p-type ZnO grown by molecular beam epitaxy”, *Appl. Phys. Lett.*, vol. 81, pp. 1830-1832, 2002.
36. K.-K. Kim, H.-S. Kim, D.-K. Hwang, J.-H. Lim, S.-J. Park, “Realization of p-type ZnO thin film via phosphorus doping and thermal activation of the dopant”, *Appl. Phys. Lett.*, vol. 83, pp. 63-65, 2003.
  37. Y.-K. Tseng, C.-J. Huang, H.-M. Cheng, I.-N. Lin, K.-S. Liu, I.-C. Chen, “Characterization and field-emission properties of needle-like zinc oxide nanowires grown vertically on conductive zinc oxide films”, *Adv. Funct. Mater.*, vol. 13, pp. 811-814, 2003.
  38. Y. W. Zhu, H. Z. Zhang, X. C. Sun, S. Q. Feng, J. Xu, Q. Zhao, B. Xiang, R. M. Wang, D. P. Yu, “Efficient field emission from ZnO nanoneedles arrays”, *Appl. Phys. Lett.*, vol. 83, pp. 144-146, 2003.
  39. H. Z. Zhang, R. M. Wang, Y. W. Zhu, “Effect of adsorbates on field-electron emission from ZnO nanoneedles arrays”, *J. Appl. Phys.*, vol. 9.
  40. H.-W. Ryu, B.-S. Park, S. A. Akbar, W.-S. Lee, K.-J. Hong, Y.-Jin Seo, D.-C. Shin, J.-S. Park, G.-P. Choi, “ZnO sol-gel derived porous film for CO gas sensing”, *Sens. Actuator B*, vol. 96, pp. 717-722, 2003.
  41. G. S. Trivikrama Rao, D. Tarakarama Rao, “Gas sensitivity of ZnO based thick film sensor to NH<sub>3</sub> at room temperature”, *Sens. Actuator B*, vol. 55, pp. 166-169, 1999.
  42. X. L. Cheng, H. Zhao, L. H. Huo, S. Gao, J. G. Zhao, “ZnO nanoparticulate thin film: preparation, characterization and gas-sensing property”, *Sens. Actuator B*, vol. 102, pp. 248-252, 2004.
  43. G. Sberveglieri, “Recent developments in semiconducting thin-film gas sensors”, *Sens. Actuator B*, vol. 23, pp. 103-109, 1995.
  44. Q. Wan, C. L. Lin, X. B. Xu, T. H. Wang, “Room-temperature hydrogen storage characteristics of ZnO nanowires”, *Appl. Phys. Lett.*, vol. 84, pp. 124-126, 2004.
  45. X. Wang, Y. Ding, C. J. Summers, Z. L. Wang, “Large-Scale Synthesis of Six-Nanometer-Wide ZnO Nanobelts”, *J. Phys. Chem. B*, vol. 108, pp. 8773-8777, 2004.
  46. H. T. Ng, B. Chen, J. Li, J. Han, M. Meyyappan, “Optical properties of single-crystalline ZnO nanowire on m-sapphire”, *Appl. Phys. Lett.*, vol. 82, pp. 2023-2025, 2003.
  47. D. F. Liu, D. S. Tang, L. J. Ci, X. Q. Yan, Y. X. Liang, Z. P. Zhou, H. J. Yuan, W. Y. Zhou, G. Wang, “Synthesis and Strong Blue-Green Emission Properties of ZnO Nanowires”, *Chin. Phys. Lett.*, vol. 20, pp. 928-931, 2003.
  48. S. C. Lyu, Y. Zhang, H. Ruh, H.-J. Lee, H.-W. Shim, E.-K. Suh, C. J. Lee, “Low temperature growth and photoluminescence of well-aligned zinc oxide nanowires”, *Chem. Phys. Lett.*, vol. 363, pp. 134-138, 2002.
  49. Z. Fan, P. Chang, E. C. Walter, C. Lin, H. P. Lee, R. M. Penner, J. G. Lu, “Photoluminescence and polarized photodetection of single ZnO nanowires”, *Appl. Phys. Lett.*, to be published.
  50. M. H. Huang, S. Mao, H. Feick, H. Yan, Y. Wu, H. Kind, E. Weber, R. Russo, P. Yang, “Room-Temperature Ultraviolet Nanowire Nanolasers”, *Science*, vol. 292, pp. 1897-1899, 2001.
  51. M. Law, D. J. Sirbuly, J. C. Johnson, J. Goldberger, R. J. Saykally, P. Yang, “Nanoribbon Waveguides for Subwavelength Photonics Integration”, *Science*, vol. 305, pp. 1269-1273,

2004.

52. H. Kind, H. Yan, B. Messer, M. Law, P. Yang, "Nanowire Ultraviolet Photodetection and Optical Switches", *Adv. Mater.*, vol. 14, pp. 158-160, 2002.
53. K. Keem, H. Kim, G.-T. Kim, J. S. Lee, B. Min, K. Cho, M.-Y. Sung, S. Kim, "Photocurrent in ZnO nanowires grown from Au electrodes", *Appl. Phys. Lett.*, vol. 84, pp. 4376-4378, 2004.
54. K. Rode, A. Anane, R. Mattana, J.-P. Contour, "Magnetic semiconductors based on cobalt substituted ZnO", *J. Appl. Phys.*, vol. 93, pp. 7676-7678, 2003.
55. Y. M. Cho, W. K. Choo, H. Kim, D. Kim, Y. Ihm, "Effect of rapid thermal annealing on the ferromagnetic properties of sputtered  $Zn_{1-x}(Co_{0.5}Fe_{0.5})_xO$  thin films", *Appl. Phys. Lett.*, vol. 80, pp. 3358-3360, 2002.
56. Y. Q. Chang, D. B. Wang, X. H. Luo, X. Y. Xu, X. H. Chen, L. Li, C. P. Chen, R. M. Wang, J. Xu, D. P. Yu, "Synthesis, optical, and magnetic properties of diluted magnetic semiconductor  $Zn_{1-x}Mn_xO$  nanowires via vapor phase growth", *Appl. Phys. Lett.*, vol. 83 pp. 4020-4022, 2003.
57. K. Ando, H. Saito, Z. Jin, T. Fukumura, M. Kawasaki, Y. Matsumoto, H. Koinuma, "Large magneto-optical effect in an oxide diluted magnetic semiconductor  $Zn_{1-x}Co_xO$ ", *Appl. Phys. Lett.*, vol. 78 pp. 2700-2702, 2001.